Article

Monitoring of Suspended Sediment Mineralogy in Puerto-Rican Rivers: Effects of Flowrate and Lithology

Trevor J. Mackowiak and Nicolas Perdrial * ◉

Department of Geography & Geosciences, University of Vermont, Burlington, VT 05405, USA
* Correspondence: nicolas.perdrial@uvm.edu

Abstract: Climate change induced changes in river flow dynamics have the potential to change the composition of suspended sediments in crucial tropical river ecosystems, possibly affecting their resiliency. This study investigates how changes in river discharge and bedrock lithology affected the physiochemical nature of river suspended sediments over a typical year in three Puerto-Rican rivers. Suspended sediment samples were collected on filter membranes in 2006 from three watersheds of differing lithology (quartz-diorite, volcaniclastic, and mixed lithology) in the Luquillo Mountains, Puerto-Rico. By monitoring changes in suspended sediment mineralogical composition (determined by XRD and SEM) as a function of discharge, we determined how sediment loads responded to changes in hydrological input in a typical year. Results showed that bedrock lithology influenced river suspended sediment mineralogy, with the fraction of crystalline versus amorphous material strongly influenced by the dominant lithology of the watershed. Crystalline phases were associated with granodiorite bedrock compared to amorphous material dominating the volcaniclastic watersheds. Thus, the mineralogy of suspended sediments in the river systems was controlled by secondary minerals. Mineralogical results showed that, bearing quantitative changes upon hydrological events, suspended sediments in all three watersheds returned to baseline composition post storm events, suggesting that the three watersheds are resilient to the events recorded that year. While the long-term mineralogical analysis of the evolution of suspended material in the studied rivers provided insights into river response to hydrologic events, it also proved technically challenging as materials in suspension in such pristine rivers are sparse and poorly crystalline.

Keywords: Luquillo; quantitative XRD; Puerto-Rico; SEM-EDS; resilience; discharge

1. Introduction

Making up only 3% of Earth's landmass, small oceanic islands contribute a disproportionate amount of nutrient to the world's oceans (e.g., 17%–35% POC, [1]). This is of particular importance in the Caribbean region, known to host the most intense weathering rates in the world [2]. Climate change modeling predicts that the Caribbean will be prone to more intense weather events likely to disturb river dynamics [3] as was already observed in recent years with the effects of hurricane Irma and Maria in 2017. While small catchments in Puerto Rico have been shown to be quite resilient to extreme events [4], increasing stress on these systems has the potential to overcome resilience threshold and fundamentally alter sediment dynamics in these systems. In order to provide a baseline to suspended sediments dynamics in small tropical catchments, we monitored the mineralogical response of suspended sediments to changes in flowrates over one year (2006) in three rivers of contrasting lithologies in the El Yunque National Forest in Northeastern Puerto Rico.

As a consequence of human induced climate change, the frequency and intensity of extreme storm events is forecasted to increase in the tropics [5]. As it is predicted that higher global temperature will trigger extended periods of dry conditions followed by intense rewetting events [6], the Caribbean region is expected to be one of the most prominent climate change hotspots in the tropics [3]. The alteration in both temperature and

precipitation are the most important physical effects of change affecting river ecosystems [7]. Because river sediments play a decisive role for riparian and costal ecosystem quality and functions [8], understanding the effects of flowrate altering events on suspended river sediments composition and quantity is fundamental to predict river ecosystem responses. Here, we discuss the results of the monitoring of suspended river sediments over one year in three Puerto-Rican rivers of differing geological settings. By monitoring the response of suspended material mineralogical and geochemical characteristics to changes in river discharge, we analyzed the effects that watershed bedrock geology have on suspended sediment in tropical river systems subjected to intense climatic events.

With ca. 15 Gt of river suspended sediments reaching the oceans every year, rivers contribute up to 95% of all sediments entering the ocean [9]. Suspended particles transported by rivers are typically clay to silt size and composed of resistant primary minerals (e.g., quartz, phyllosilicates and zircon), secondary minerals (clays, metallic oxides and oxyhydroxides) and biogenic remains which can be transported either as bed load or fine-grained suspended particles [10,11]. By means of transporting materials from erosion areas (mountains) to sedimentation basins (oceans), rivers are the principal conveyor of dissolved and solid-laden essential nutrients, such as Ca, Na, and K [12,13], and constitute the principal contributor to ecosystems' nutrient cycling from terrestrial systems to oceanic systems [14]. Tropical rivers contribute 38% of the dissolved ions and 65% of dissolved silica to the Earth's ocean's while only covering 25% of the Earth's surface [15]. As such, tropical rivers contribute much more mass than other comparable ecosystems due to the high temperature and surface runoff that leads to fast weathering rates [16,17]. Because of the typical smaller size of these catchments, the rate at which the bedrock weathers and the byproducts of weathering are largely dependent on the bedrock lithology of the localized areas [15,18]. Nonetheless, high weathering rates associated with mountainous tropical catchments typically yield fairly mature sediments in these rivers, dominated by weathering-resistant primary minerals (e.g., quartz) and advanced secondary minerals (e.g., kaolinite) as highlighted by numerous studies [4,11,19–21]. The scale of the watershed also controls the amount and nature of the weathering product transported in the river: close to headwaters, immature products dominate while near the mouth of the river, sediments tend to be more mature ([22] and references therein).

Increasing anthropogenic activity is dramatically impacting river sediment fluxes throughout the world. Climate change and human activities have been shown to have major effects on the nature and amount of sediments carried by rivers. Examining the changes in water and sediment fluxes and their drivers for over four thousand large rivers worldwide, Li et al. [23] found that 24% of the world's large rivers experienced significant changes in water flux and 40% in sediment fluxes due to climate change and human impacts. As they are highly sensitive to the seasonality of the intertropical convergence zone [24], tropical river systems are especially vulnerable to the effects of climate change because of the predicted increase of intensity of storms in the tropics [5]. Due to an increase of greenhouse gasses, the atmosphere becomes warmer and is able to hold more moisture. This results in increased periods of drought followed by intense storm events that rewet the surface [25]. During periods of drought river systems discharge is low, resulting in transport of small sediment particles and deposition of larger sediments. An intense storm following a period of drought can drastically change the composition of suspended sediments in river systems. During the initial influx of discharge from the storm, small particles previously deposited on the river bed are flushed from the system. With successive storm events, the source of suspended sediment is the river bank rather than the river bed because all of the small particles have left the system. These small particles will reaccumulate with time. The increased frequency of droughts and floods in tropical regions leads to economic and ecological impacts including damages to infrastructure [26]. Peak rates of hydrological fluxes (high and low) observed in islands of the Caribbean have proven to be some of the most extreme values in the world for the size of the islands' watersheds and are likely to

continue to display exceptional discharge values due to projected regional manifestations of global climate change [27].

Previous research by Clark et al. [4] analyzed the mineralogy of the suspended sediment in two Puerto Rico river systems with differing bedrock lithology across four rain events following an extreme drought. The study found both river systems to be resilient to extreme droughts. However, differing lithologies responded differently to rewetting events: suspended material in the river system draining volcaniclastic bedrock decreased in crystalline quartz minerals after successive rain events, whereas the amount of quartz increased linearly with every storm event in the river draining granodiorite bedrock [4]. This was explained by differences in sediment sources linked to the nature of weathering products in the rivers.

To provide a base line for the study of tropical river response to extreme climatic events, we analyzed the evolution, over a year, of suspended sediment mineralogy and chemistry in three small tropical Puerto Rican rivers, Rio Mameyes, Rio Icacos, and Quebrada Sonadora. These catchments have been chosen because they are pristine watersheds presenting contrasted bedrock conditions (granodiorite vs. volcaniclastic [4,28]) and practically identical climates [29]. These conditions allow for differences in river system response to changes in precipitation caused by the differing bedrock lithology underlying the watersheds to be studied and compared. Using X-ray diffraction (XRD) and scanning electron microscopy with electron dispersive spectroscopy capabilities (SEM/EDS), we determined how the mineralogical composition of suspended sediment differed in the different tropical river systems across a year and determined how differing lithologies affected the rivers dynamical responses. To test the hypothesis of Clark et al. [4] that flow-related differences in sediment sources influenced the composition of suspended sediments, we characterized streambed and streambank sediments in each watershed.

2. Materials and Methods

2.1. Sampling Area

Three river catchments were studied: Quebrada Sonadora (QS), Rio Mameyes at Puente Roto (MPR), and Rio Icacos (RI). All catchments (Figure 1) are part of the El Yunque National Forest, Puerto Rico, and part of the Luquillo Critical Zone Observatory (LCZO) and Luquillo Long Term Ecological Research (LTER). El Yunque National Forest is located in northeastern Puerto Rico. The dominant feature of the forest is the Luquillo Mountains, which rise to 1077 m above sea level. Rainfall in the area ranges from an average of 3537 mm/year at low elevations to 4849 mm/year higher up and average temperatures are around 23.5 °C in the winter and 27 °C in the summer [30]. The topography of the watersheds in this region is narrow and steep, causing them to respond quickly to changes in precipitation [31]. The bedrock in the area consists principally of the Paleogene Rio Blanco quartzdiorite and Cretaceous volcaniclastic rocks (Figure 1 [32]). The Rio Blanco diorite consists principally of plagioclase, quartz, amphibole, and minor biotite [33]. Its weathering happens spherically [34,35] leaving corestones weathering into an Inclusive saprolite [31]. This saprolite is principally composed of quartz, weathered mica, kaolinite and other clays [31] and is covered with 0.5–2 m of sandy soil [36]. The volcaniclastic rocks are principally composed of glassy rock fragments and associated plagioclase, pyroxenes, and rare quartz grains [31,37]. The saprolite forming from this bedrock is rich in kaolinite, iron and aluminum oxides, and small amounts of quartz [31]. Soils overlying these terrains are typically clay-rich and quartz-poor. The drainage area before the gage at MPR is 17.8 km^2 [31] and is underlain by 80% Cretaceous volcaniclastic bedrock and 20% quartzdiorite. The drainage area before the gage at RI is 3.26 km^2 [31] and flows over 100% Rio Blanco quartz diorite bedrock [4]. The drainage area before the gage at QS is 2.6 km^2, and flows over 100% cretaceous volcaniclastic bedrock [38]. As such, RI represents a quartzdiorite endmember, QS a volcaniclastic endmember, and MPR a mixed lithology watershed.
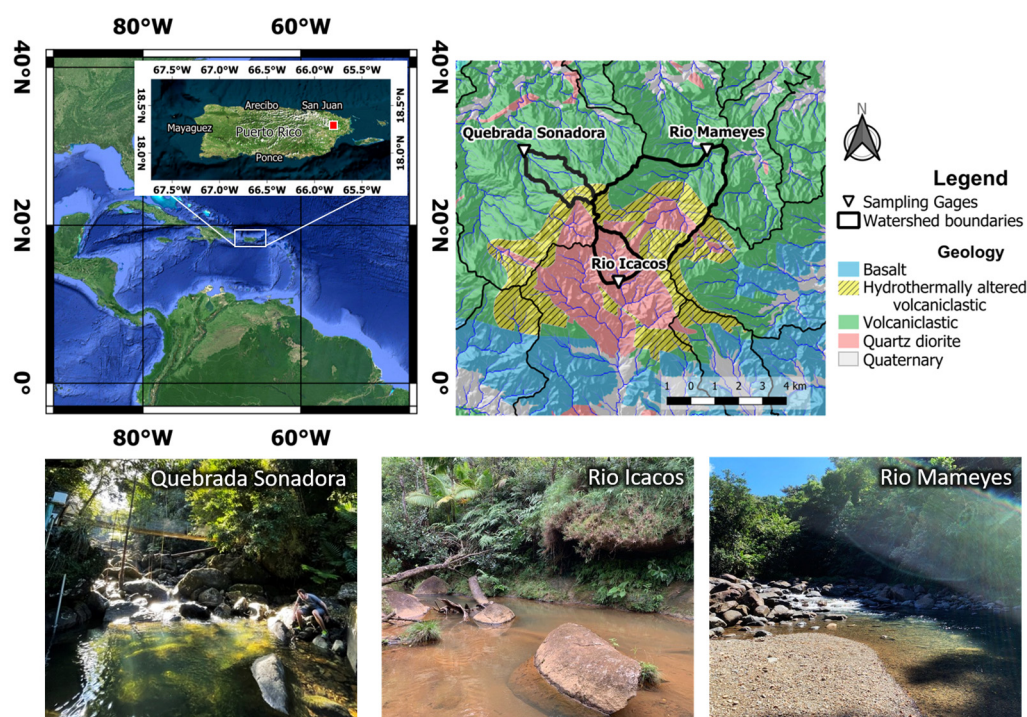
Figure 1. Location, geology, and representative pictures (at low flow) of the studied watersheds. Red square on inset map corresponds to the area on the geologic map (Geology based on Seiders et al. [32]).

2.2. Stream Discharge Measurments

USGS stream discharge monitoring was performed for MPR, RI, and QS from 1991-present, 1992-present, and 1999 to 2010 respectively, and was used here to study the relationship between suspended sediments and discharge. For the year of this study, 2006, the stream discharge data were measured in 15-min intervals by recording stage height and converting to discharge using a stream stage/discharge equation (USGS, 2019). Data were accessed through the USGS website (waterdata.usgs.gov, 19 December 2022).

2.3. Suspended Sediments Collection

Suspended sediment samples were collected at MPR, RI, and QS in 2006 at USGS stream discharge gages as part of the LCZO monitoring campaigns. Suspended sediment samples were collected by passing 1000 mL of water from each respective stream through 0.45 μm filter membranes. Water samples were collected weekly, except during extreme weather conditions or road closures that prevented sampling. Filters were individually packaged and stored at University of New Hampshire (UNH) in dry state in the dark. After sampling, samples were analyzed for C and N content at UNH. Here, we analyzed the filters for physical characteristics, including particulate color, assessment of suspended sediment filter coverage, crystalline composition, major elements composition, and microscale physicochemical characteristics of the suspended matter (Table S1a–c).

2.4. Sediment Grab Collection

Because different pools of sediments are expected to be mobilized at different flowrates, we characterized the nature of sediments in the streambeds and the streambanks of the three rivers. Streambed sediments are representative of sources mobilized at low flow, while streambank sediments, located above the river base level are only mobilized during high flow events. In January 2022, six sediment samples were collected close to the monitoring gage from each watershed. In each river system, three samples of ca. 20 g of sediments were collected from the river bottom and three samples were collected from the bank of the

river approximately 15 cm up from where the water level of the river meets the bank at baseflow. Bottom sediment samples were collected by inserting a 100 mL wide mouth bottle at a 45-degree angle approximately 3 cm into the sediment surface. The bottle was tilted horizontally and then vertically and lifted out of the water. The water sediment mixture was transferred to a bag, left to settle overnight, and more excess water was poured out of the sample bags in the morning. Bank sediments were sampled in dry state. The sediment samples were then shipped back to the University of Vermont where they were air dried at room temperature for 7 days (Table S1a–c). While the river sediments were collected in 2022 and the suspended sediments in 2006, good stream resilience in the area [4] suggests that the nature of streambed and streambank sediments did not change drastically in these 16 years.

2.5. Sediment Size Analysis

The sediment size distribution of the air-dried river sediment samples collected during January 2022 field work was determined by sieving through 2-mm, 500-µm, and 63-µm sieves. The sieves were mechanically shaken for 45 seconds, and separated sediments were placed into individual bags. The mass of each sediment size was recorded.

2.6. Filters Physical Characterization

Filter membranes with suspended sediment collected in 2006 were visually analyzed for physical characteristics including color, texture, and thickness. The color of the sediment was used as a relative indicator for matter present in the suspended sediment at the time of collection. Collected suspended sediment color ranged from very pale orange to moderate brown. The texture of the suspended matter was also visually observed and compared to other samples collected throughout the year. The suspended matter on the filter membranes was analyzed for its relative thickness by visual observation. To ensure accurate comparison of the filters color, all filter membranes were photographed in identical light conditions.

2.7. Mineralogical Characterization

To characterize and quantify the nature and amount of crystalline material present in the suspended sediment, filter membranes and collected sediments were analyzed by powder X-ray diffraction (XRD) using a Rigaku MiniFlex II, equipped with a Cu X-ray tube. Suspended sediment samples were left on the filter membranes and mounted flat on a glass slide before being placed into the diffractometer. Air-dried 2 mm sieved sediment grab samples from the riverbeds and riverbanks of the three rivers were ground to a powder, mounted unoriented onto a glass slide and inserted into the diffractometer. Approximately 2 g of the riverbed and riverbank sediments were subjected to <50 um extraction protocol by sonicating the sediments in ethanol before settling according to Stoke's law, following the protocol described in Perdrial et al. [39]. The resulting fine fraction was pipetted onto a glass slide to allow for platy particles to preferentially orient during drying. Analysis was carried out in 2theta-theta geometry between 3 and 70°2θ with a dwelling time of 1°/min. Diffractograms were analyzed qualitatively using the ICDD 2.0 and COD databases for peak matching. Quantitative analysis of the X-ray diffractograms was performed using a semi-automatic Rietveld approach [40] in the whole pattern profile fitting module of the PDXL-2 software. Parameters allowed to vary were scale factor, cell parameters (within 0.2Å), shape parameters, and for selected minerals (clays and amphiboles) the preferred orientation March–Dollase parameter. While results of the quantification are provided here, with strong goodness of fit, it is important to note that quantification of the fine fraction is to be interpreted with care because of the combination of high preferred orientation and the high background inherent to the small thickness of the extracted samples.

2.8. Elemental Characterization

Suspended sediment Al and Fe composition was quantified using a portable X-ray fluorescence (XRF, Hitachi X-MET8000). Suspended sediments on their respective filter

membrane were analyzed for 60 s in triplicate directly on the filter, with the side covered with sediment facing the detector. All results reported represent an average of the triplicate measurements and error is expressed as one standard deviation. Additionally, a National Institute of Standards and Technology standard reference material (NIST 2709a) was analyzed and compared to certified values with the following recovery values of target elements: Al at 88%, and Fe at 107%. While blank filters analyzed by XRF contained significant amounts of other elements (e.g., Mg, Si, K, Ca), they did not contain any significant amounts of Al and Fe.

2.9. Physico-Chemical Characterization of Selected Suspended Matter

Scanning electron microscope (SEM) images and associated electron dispersive spectroscopy (EDX) spectra of selected suspended sediment filters were acquired to identify the structure and chemical composition of particles comprising the suspended sediments. Samples were selected based on date, discharge, and river catchments. For each site, two samples were analyzed using a ZEISS SIGMA SEM equipped with an Oxford EDS attachment. One sample was collected in the winter months as representative of low flow $(0.06–1.5 \text{ m}^3/\text{s})$ conditions, the other sample was collected in May 2006 after a high flow event for all three rivers $(11.33–15.57 \text{ m}^3/\text{s})$. A small triangle was cut out of each selected filter membrane and placed onto carbon tape attached to an aluminum SEM mount. Mounted samples were then sputter coated in a 60:40 Pd:Au mix to improve conductivity as needed for EDS analysis. Sputter coated samples were then placed in the SEM and analyzed in SE mode at 20 kV EHT and 8.5 mm working distance. Maps showing the relative Al, C, Fe, and Si were created using AZtecLive™ software. First an overview image of the sample was created at low magnification (100×). A site of interest was then selected from the overview image and magnification was increased in that area (300–600×). For all images, an EDS map was acquired with a counting time of 4 min. Two sites of interest were selected for each analyzed sample. This process was repeated for each sample analyzed.

3. Results

3.1. River Discharge and Sediment Loadings

Due to differences in watershed areas, river discharge values for the three sites differed in intensity. However, periods of high discharge occurred on the same dates due to the close proximity of the three rivers. Over the year, a number of rain events resulted in increased discharge events in the streams (Table S2 and Figure 2). While each stream's major discharge event happened on a different date, all streams experienced significant high discharge events on or around 5 April. While these peak flow events reflect episodic events (Table S2a), average daily high flow events represent longer stream response to precipitation (Table S2b). Here, long-term flow events impacted all three streams around 10 July, and 22 April (Table S2 and Figure 2). Two dry periods contributed to low discharge in all three streams: between 19 February to 6 March and between 17 May and 27 May (Storm events database, 2021 and Figure 2). We attribute differences in the ranking of events between rivers to the fact that the size of watersheds varies and the fact that each watershed has different aspects: QS is NW facing, MPR is NE facing and RI is SE facing (Figure 1).

Analysis of the color of the particulate matter on the white filters provided a proxy for sediments loading over the sampling period. RI filters were generally darker than MPR and QS. At MPR, loading was generally low (light colors) except for the January and October samples (Figure 2). At RI, loading appeared high and homogeneous over the sampling period (Figure 2). QS loadings were highly variable over the sampling period (Figure 2).
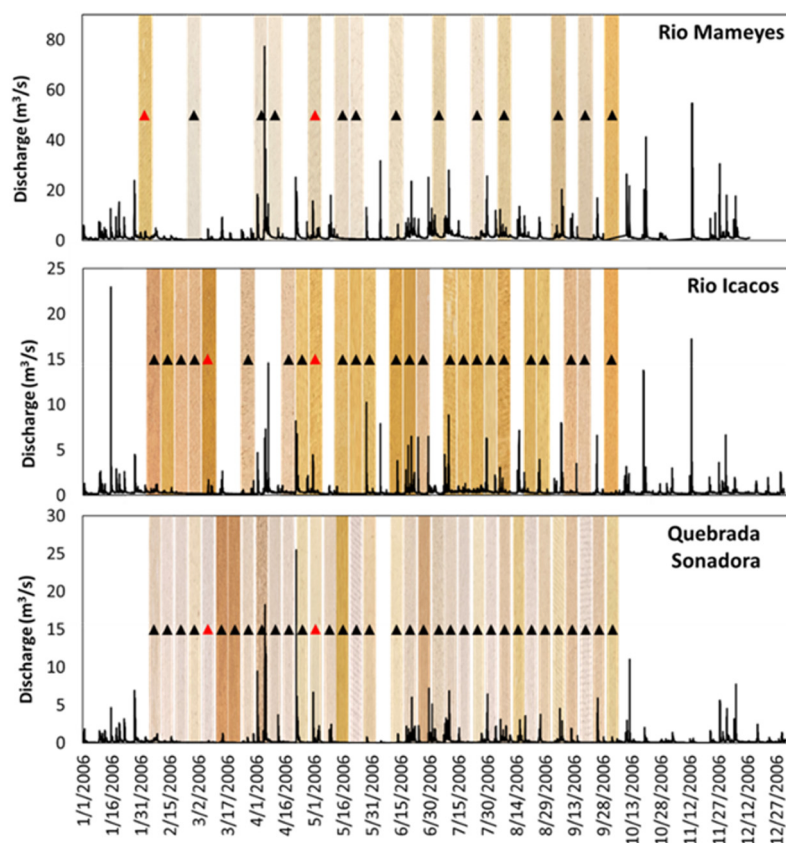
Figure 2. River hydrographs overlain on cropped images of collected filters (vertical yellow-brown bars) for respective river and sampling date. Black triangles represent a date of sample collection, and red triangles indicates sample has been analyzed with SEM-EDS (date format: MM/DD/YYYY).

3.2. Texture and Mineralogy of Streambed Sediments

3.2.1. Texture

At all three rivers, sediments collected from the river bottom contained more large sand size grains (>2 mm) than the samples collected from the river bank (Figure S1). Sediments collected from the river bottom at QS contained the highest percentage of sand size sediments (>2 mm) out of the three river systems (Figure S1), while samples collected from the bank of RI contained a larger relative fraction of small particles (<500 μm, Figure S1).

3.2.2. Mineralogy

Sediments collected from the riverbed of the MPR and RI are similar in composition, dominated by quartz, plagioclases, and amphiboles while riverbed sediments in QS are principally composed of plagioclases, kaolinite, a 14Å phase, and a mixture of accessory minerals labelled as "other" and principally consisting of pyroxenes and possible pyrite (Figures 3 and S2). Riverbank sediment composition show this difference in a less pronounced manner with similarities in quartz, plagioclases, and amphibole content between MPR and RI but an important contribution from kaolinite in RI samples. The composition of the QS riverbank sediment is similar to the riverbed one (Figures 3 and S2).

Fine fraction (<50 μm) extracts are largely dominated by kaolinite in all three rivers in both the riverbed and riverbank sediment pools (Figures 3 and S3). These mineralogical signatures reflect both the differences in watershed geological makeup and intense weathering reactions affecting the rocks in this tropical setting. The broadness of diffraction peaks, associated with low quartz peak intensity at QS, is a direct reflection of the volcaniclastic nature of the bedrock while the significant fraction of quartz, plagioclase and amphibole at RI and MPR is a clear reflection of the presence of quartz-diorite in

the watershed (Figures 3 and S3). The lesser relative amount in quartz and plagioclase at the expense of weathering products (kaolinite, 14Å phase and gibbsite) in the riverbank sediments reflects a lower amount of hydrologic sorting in riverbank sediments compared to riverbed sediments.

In relation to the hypothesis that flow-related differences in sediment sources influenced the composition of suspended sediments, these distinctive characteristics in sediment pools provide interesting fingerprinting to interpret the sourcing of suspended particles in the rivers.
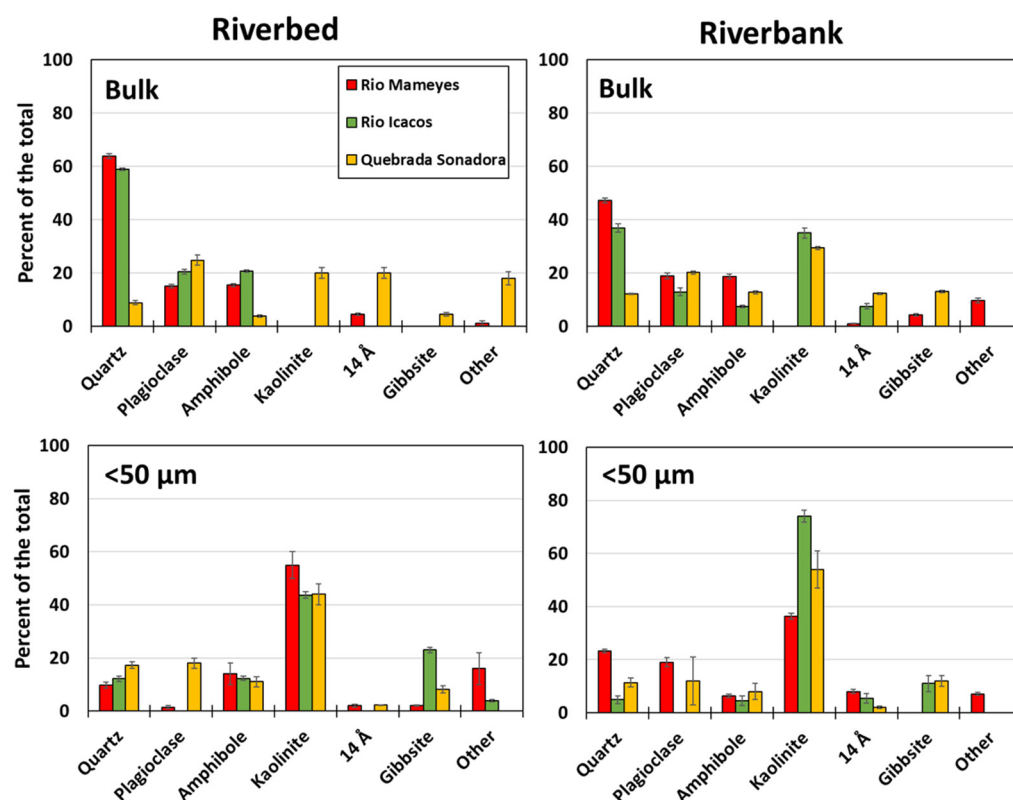

Figure 3. Relative mineralogical composition of river sediment grab samples collected in February 2022. Bulk correspond to the bulk composition and <50 μm to the composition of the <50 μm concentration. Results are from the Rietveld refinement of diffractograms presented on Figures S2 and S3.

3.3. Mineralogy of Suspended Sediments

The general lack of well-defined peaks in the diffractograms of filters reveals that MPR suspended sediments were dominated by amorphous material (Figure 4). At MPR, filters collected on 2/7/2006, 7/5/2006, and 8/8/2006 had notably more crystalline material than other filters (Figure 4A). This crystalline material was composed of a 14Å phase, kaolinite, and quartz. Overall, MPR showed the least evidence of crystalline material across all three rivers (Figure 4). The positions of diffraction peaks of suspended sediments collected at RI were consistent across the monitoring period pattern with varying degrees of intensity (Figure 4B). Of the 25 suspended sediment samples, only the four filters collected at the beginning and middle of May, beginning of July, and beginning of August lacked crystalline structure. Crystalline minerals were dominantly kaolinite and quartz with the addition of small amount of a 14Å phase. Overall, RI has the most crystalline material in the suspended sediment samples across all three rivers (Figure 4). Similar to MPR, the diffractograms of suspended sediment samples collected at QS revealed some filters devoid of crystalline materials (2/7/2006 to 2/28/2006, 3/28/2006 to 5/2/2006, and 6/27/2006 to 8/29/2006, Figure 4C). The remaining samples contained various amounts of 14Å chlorite-like phase, kaolinite, and quartz. Samples collected on 3/7/2006 and 3/14/2006 had comparably more crystalline material than the other filters.
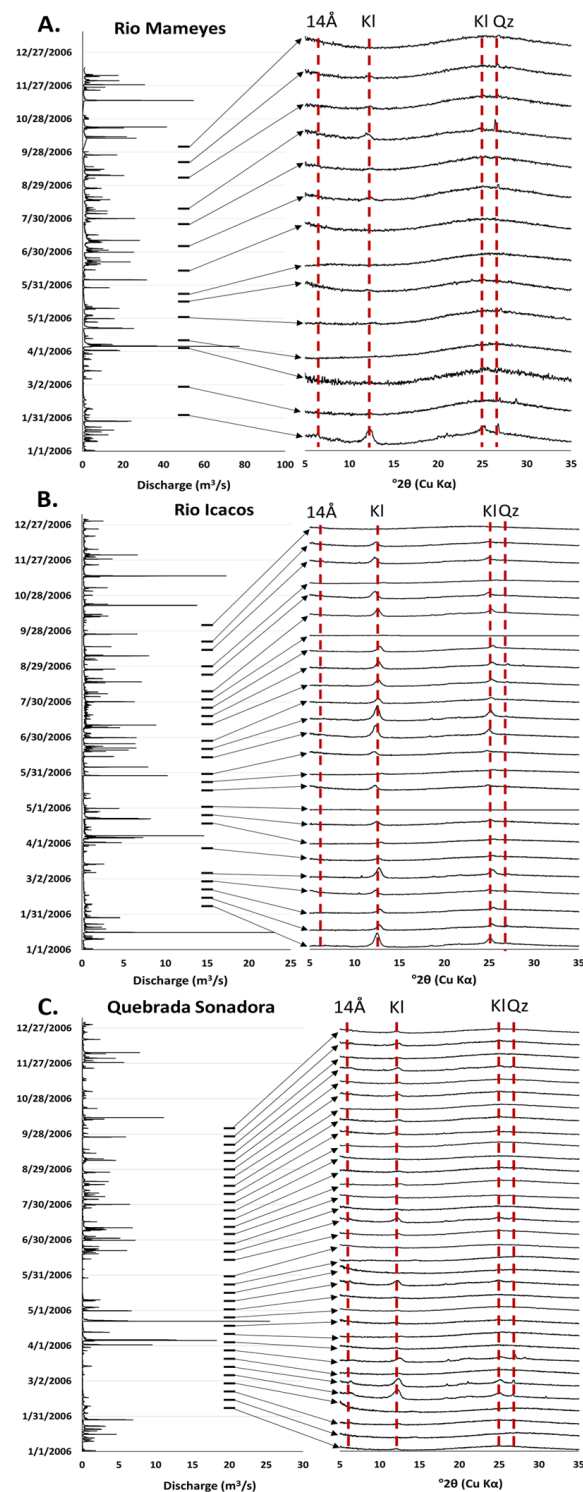
Figure 4. Hydrographs and X-ray diffractograms for Rio Mameyes (**A**), Rio Icacos (**B**) and Quebrada Sonadora (**C**). XRD Diffractograms of suspended sediment samples on filters are ordered by sample collection date (connected with arrows, date format: MM/DD/YYYY) red dashed lines indicate the main mineral peaks. Date labels by the diffractograms identify diffractograms mentioned in the text Section 3.3. Mineral abbreviations (14Å: chlorite-like, Kln: kaolinite, Qz: quartz) are from Warr [41].

3.4. Fe and Al Composition of Suspended Sediments

Fe and Al concentrations were variable across streams and consistently correlated one with the other (Figure 5). At RI and QR, increases in Fe and Al concentrations were

observed during extended periods of low flow (February to March and June, Figure 5). At MPR, however, extended periods of low flow contributed to a sharp decrease in Fe concentrations (February and mid-May, Figure 5).
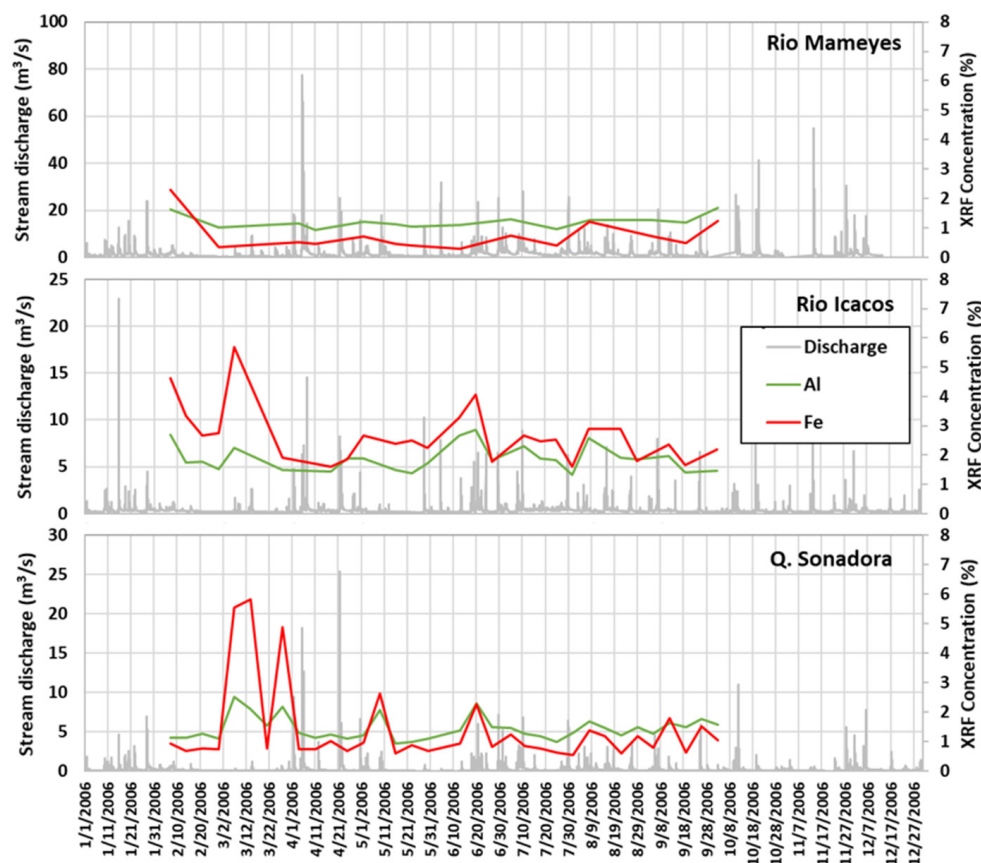

Figure 5. River discharge and concentrations from XRF analysis in percent of Al and Fe of suspended sediments collected on filters.

3.5. Physical and Chemical Nature of Suspended Sediments

The SEM/EDS images of the filter membrane collected on 2/7/2006 at MPR (a sample acquired after a representative low flow period) is covered (caked) in material composed primarily of Al (Figure 6A). Individual particles are principally nanometric to micrometric Al and Si rich with some larger (50–100 μm) Al rich aggregates containing Fe and C (Figure 6B). The filter collected on 5/2/2006 at MPR after a high flow event shows much less particulate coverage with disseminated small (a few μm in diameter) Al-rich and Si-rich particles (Figure 6C,D) and a few larger particles (diameter > 20 μm) principally composed of Al. Some aggregates of Si-Fe material and individual C-rich particles were also observed (Figure 6D).

SEM/EDS maps from the suspended sediment on the filter collected on 2/28/2006 at RI, a sample representative of a low flow period, showed a filter almost completely covered (caked) in suspended material (Figure 7A) of a few μm in diameter and principally composed of Al, with discrete Si and Fe rich particles (Figure 7B). The filter collected at RI on 5/2/2006 after a high flow event is much less covered in material consisting in a range of 5–50 μm (in diameter) Al-, Fe-, and C-rich particles with larger clay-like particles (Figure 7C,D).
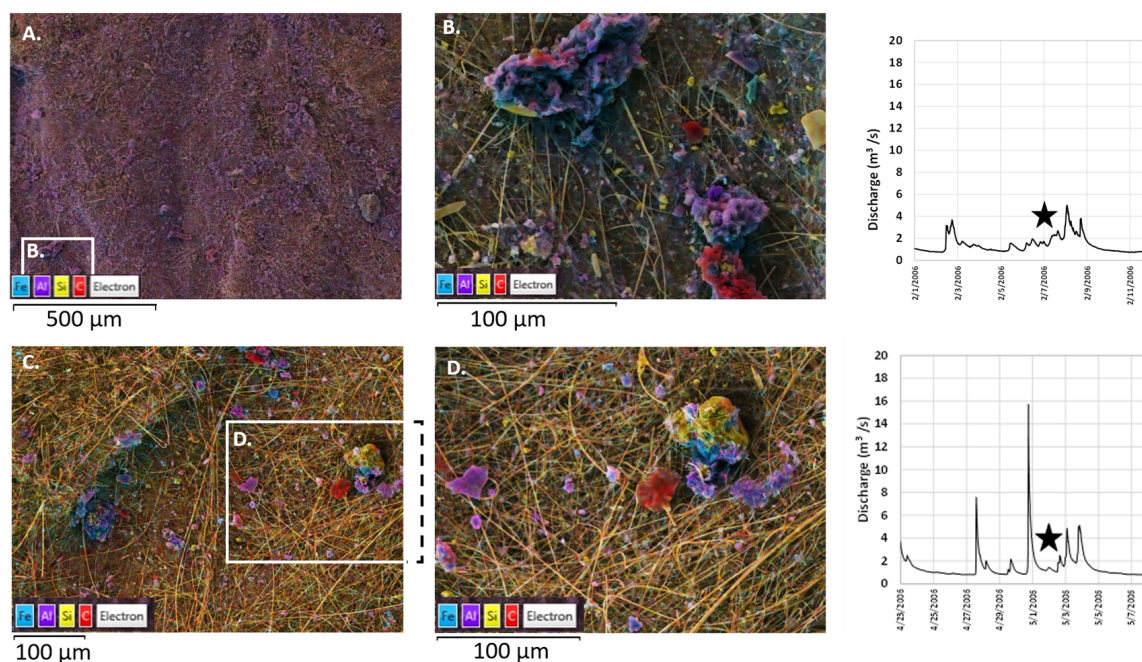
Figure 6. Representative SEM/EDS maps of selected Rio Mameyes filters under contrasted flow (as seen on the hydrographs on the right). (**A**) Low magnification composition map of overview area during low flow. (**B**) Composition map of area B in overview area A. (**C**) Low magnification image of filter collected during high flow. (**D**) Composition map of focus area D in overview area C. Si-rich fibers in the background are constituents of the filter membrane. Colors represent selected elements (Fe, Al, Si and C). Stars on the hydrographs represent the time when the corresponding filter was collected.
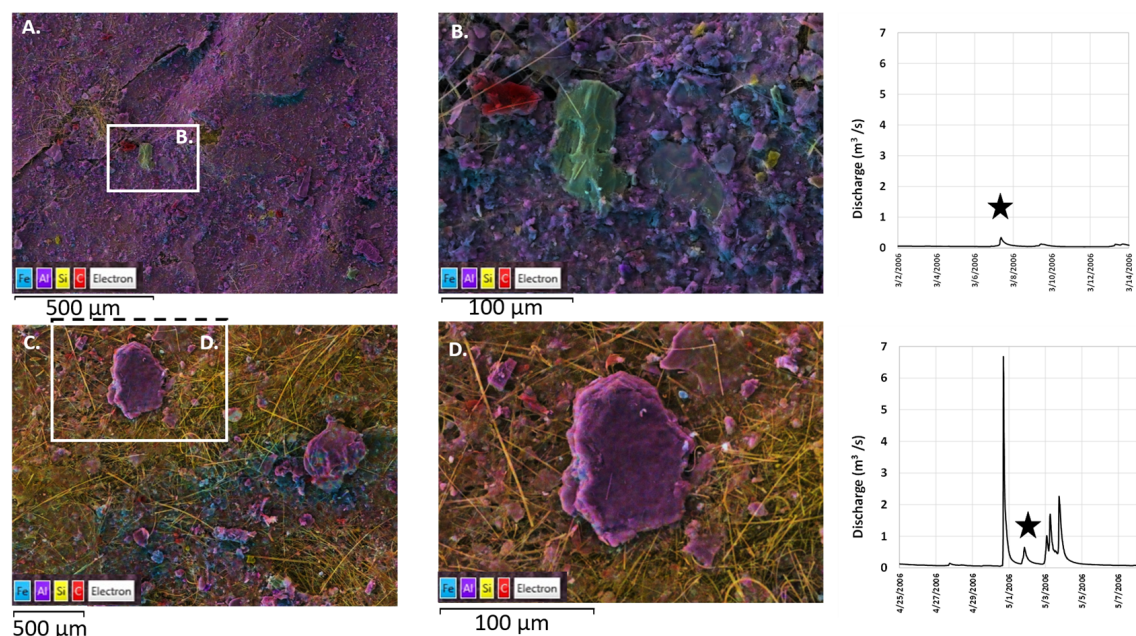

Figure 7. Representative SEM/EDS maps of selected Rio Icacos filters under contrasted flow (as seen on the hydrographs on the right). (**A**) Low magnification composition map of overview area during low flow. (**B**) Composition map of area B in overview area A. (**C**) Low magnification image of filter collected during high flow. (**D**) Composition map of focus area D in overview area C. Si-rich fibers in the background are constituents of the filter membrane. Colors represent selected elements (Fe, Al, Si and C). Stars on the hydrographs represent the time when the corresponding filter was collected.

Composition maps of the filter membranes collected on 3/7/2006 at QS, a representative sample of a low flow period, also showed a filter covered in a layer of Al-rich particles (Figure 8A). Higher magnification maps revealed that the "caked" layer is made of nano- to micrometric Al- and Fe-rich particles and some Si-rich particles with sporadic larger particles (diameter > 25 μm) composed principally of Si and C (Figure 8B). The suspended sediment collected at QS on 5/2/2006 following a high flow event is composed of large particles (diameter > 25 μm) principally composed of Al (Figure 8C). Large, sheeted, clay-like Al rich particles were frequently observed on the filter membrane (Figure 8D).
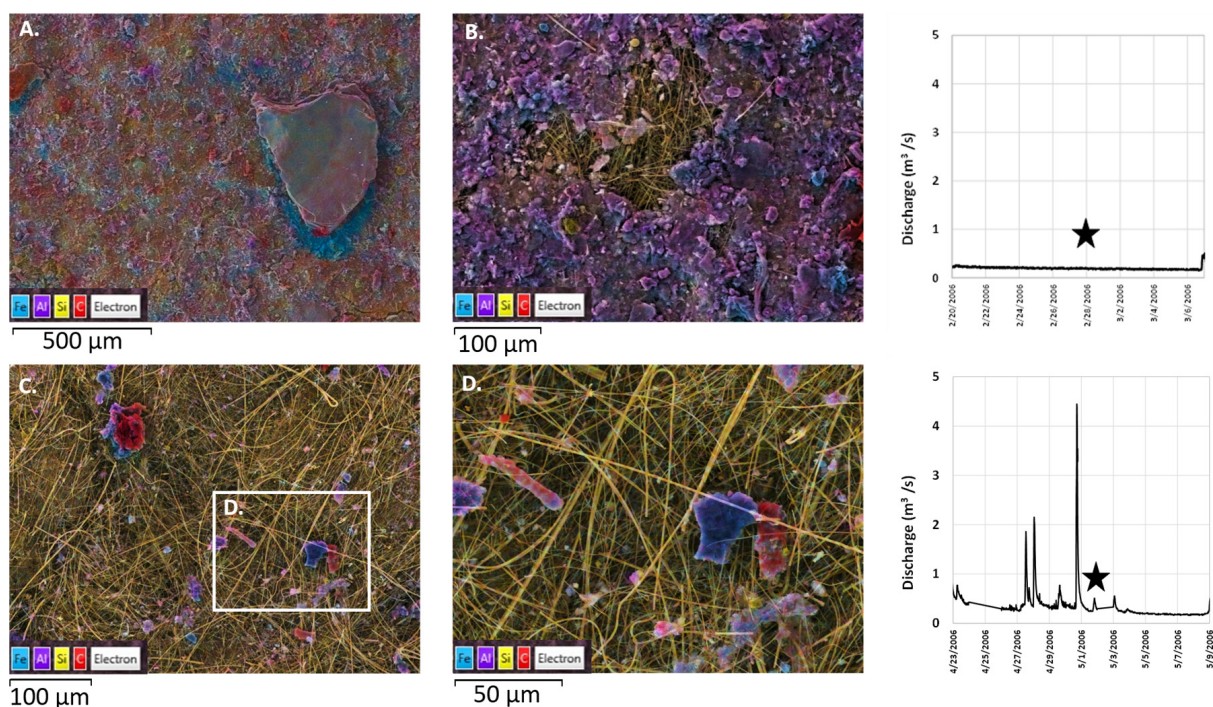

Figure 8. Representative SEM/EDS maps of selected Quebrada Sonadora filters under contrasted flow (as seen on the hydrographs on the right). (**A**) Low magnification composition map of overview area during low flow. (**B**) Composition map at higher magnification of filter in A (area not shown). (**C**) Low magnification image of filter collected during high flow. (**D**) Composition map of focus area D in overview area C. Si-rich fibers in the background are constituents of the filter membrane. Colors represent selected elements (Fe, Al, Si and C). Stars on the hydrographs represent the time when the corresponding filter was collected.

4. Discussion

4.1. Mineralogy and Sourcing of Suspended Matter across Sites

The bedrock of the Rio Icacos watershed is predominantly quartz granodiorite, that of QS is predominantly volcaniclastic, while the bedrock at MPR is a mixture of both rock types (Figure 1). This difference in bedrock composition was partially reflected in the mineralogical composition of both riverbed and riverbank sediments and suspended sediments. Sediments from the two rivers with granodiorite in their watersheds (i.e., MPR and RI) contained principally quartz, plagioclases, and amphiboles while QR contained little quartz and amphiboles (Figure 3). At RI, 12% of filters were entirely amorphous, 29% at QS, and 42% at MPR (Figure 4). When present, crystalline phases were dominated by kaolinite with some occurrences of quartz and a 14Å chlorite-like phase. Volcaniclastic rocks in the area are principally composed of glassy rock fragments and associated plagioclase, pyroxenes and rare quartz grains [31,37], which weather principally congruently with limited formation of secondary minerals. The intrusive Rio Blanco quartz granodiorite consists principally of plagioclase, quartz, amphibole, and minor biotite that weather incongruently [31]. The observation that suspended sediments were more crystalline at RI than QS and MPR is

in direct agreement with the fact that RI drains a 100% granodiorite watershed while QS and MPR are principally draining volcaniclastic bedrocks. The predominance of crystalline phases at RI is a direct reflection of the nature of the bedrock and associated stream sediments (Figure 3), where the weathering of granodiorite produces quartz-dominated arenitic sediments, and feldspars evolve into kaolinite via intense hydrolysis [4]. On the other hand, volcaniclastic bedrock is dominated by poorly crystalline and glassy phases that tend to dissolve congruently limiting the production of crystalline material in the suspended sediment as confirmed by the composition of stream sediments (Figure 3). Analysis of samples by SEM confirmed the dominance of saprolite materials in the suspended sediments with a composition dominated by Al, Si and Fe (Figures 6–8), the three most common elements with a high ionic potential and therefore the most common recalcitrant elements during weathering [42]. Similar to the observation of other rivers [11,43], aside from the difference in amorphous vs. crystalline nature of the suspended particles, no difference in composition of the suspended sediments was observed by visual color inspection, XRD, or SEM. We explain this by the fact that the composition of suspended sediments in tropical systems is heavily influenced by hydrolysis leaching occurring prior to transport. In other words, the general composition of suspended sediments is dominated by the composition of the final product of weathering. As a result, our analysis suggests that compositional analysis of suspended sediments by XRD in small tropical catchments complicates sediment sourcing analysis. Instead, we suggest that crystallinity be used as a proxy for sediment sourcing when lithology is sufficiently contrasted (e.g., basic vs. acidic rocks).

4.2. Effect of Flow on Suspended Matter

As evidenced by SEM, loads of suspended materials depended on the flow regimen prior to sampling. In all watersheds, suspended sediments sampled after a low flow period were caked with fine particles (Figures 6A,B, 7A,B and 8A,B) while suspended material sampled after a high flow event were sparser and contained larger particles (Figures 6C,D, 7C,D and 8C,D). While this clear difference did not translate to a change in filter color (Figure 2) or mineralogic composition and crystallinity patterns (Figure 4), it was reflected by changes in Fe and Al content on the filters (Figure 5). We interpret the absence of flow-impacted differences in mineralogic composition of crystalline phases to the homogeneous nature of the sediments across all three sites. As no compositional differences existed between the crystalline suspended matter across sites while variations in amorphous and crystalline matter content existed, differences in stream power impacted only the size of the suspended matter where larger, more crystalline particles remained in suspension after high flow events but not after low flow events. Comparing with the composition of bed and bank sediments, it appears that little primary mineral can be transported in the stream with most suspended material corresponding to the 50 um fraction of riverbed and riverbank sediments (Figure 3). This sorting difference is also corroborated by the evolution in Fe and Al composition of the suspended matter (Figure 5). Increases in Fe concentrations on the membranes during extended low flow periods is similar to the observation made by Knapp et al. [44]. As Fe was not particularly associated with C (SEM) in our study, we cannot explain this mobilization by organic matter–Fe interactions. Instead, we propose that Fe precipitate during low flow, due to either high evaporation events in soils [44] or increasing stream pH [45].

While events modified streams' suspended matter mineral and elemental composition in all watersheds, each of the watersheds showed resilience as the mineral and elemental compositions of the sediment remained similar across the year of monitoring.

4.3. Link to Stream Water Chemistry

Recent analysis of the lithological control of stream chemistry in the three studied watersheds by Hynek et al. [28] concluded that lithological differences, in particular fractionation patterns and susceptibility, have a major influence on stream water chemistry. Using daily stream water data spanning between 1997 and 2007, Hynek et al. [28] con-

cluded that differences in recharging flow paths in the three rivers we studied are driven by variation in lithology. Their results suggest that porosity/permeability differences between the regolith in the three watersheds control the extend of mineral dissolution. As a result, major differences occur in the chemistry of the streams, with QS stream water exhibiting low solute concentrations because of limited weathering, RI stream water exhibiting intermediate solute concentrations due to saprolite infiltration around core stones, and MPR showing high solute concentrations because of high fracture density, leading to high porosity. As applied to suspended sediments, these processes would suggest that QS sediments be the least impacted by weathering, followed by RI and MPR. Accounting for differences in lithologies, our results are partially agreeing with this picture. Indeed, suspended sediments in MPR contained very little crystalline material, suggesting intense weathering with little secondary mineral formation (Figure 4). Suspended sediments at RI were mostly crystalline, dominated by primary recalcitrant and secondary minerals (respectively quartz and kaolinite, Figure 4), which suggest intense weathering reactions. Suspended sediments at QS were however at odds with the conclusions of Hynek et al. [28]. Suspended material appeared intermediate in nature with some samples containing significant secondary minerals and other mostly amorphous (Figure 4). As QS drains 100% volcaniclastic material, containing the least amount of minerals prone to incongruent weathering among the three watersheds, and because of low solute concentrations, we suspected that this watershed would contain the least amount of secondary minerals in the suspended sediments. Instead, it appears intermediate in nature. We suspect that this is due to the differences in catchment area between MPR and QS (respectively 17.8 km^2 and 2.6 km^2), with the larger MPR catchment allowing for more hydrologic sorting and dilution of the saprolite-sourced materials.

4.4. Geology and Hydrological Event Co-Dependencies on Tropical Stream Dynamics as Reflected by Suspended Matter

Monitoring of suspended matter mineralogy as a function of discharge has seldom been carried out at high resolution. Studies on large rivers have pointed out to the importance of catchment geology and anthropogenic impacts [11,46,47]. In smaller catchments, changes in flow regimen were shown to impact the mineralogical nature of the sediments with an increase in the contribution of primary minerals during high flow events [48,49]. Analyzing the effects of individual storms on the nature of suspended matter in two of the rivers studied here, Clark et al. [4], suggested a co-dependency between hydrological events and sourcing of the sediments. Here, we didn't observe such co-dependency as the mineralogy of suspended materials could not be linked to discharge data (Figure 5). Only SEM characterization showed clear differences between low and high flow regimen with an abundance of fine particles during low flow events and larger, less concentrated particles after high flow that we attribute to hydrologic sorting (Figures 6–8). We explain this apparent contradiction by differences in sampling between our study and Clark et al. [4]. While Clark et al. [4] sampled specifically during high flow events, our samples were collected at regular weekly intervals. As such, our observations are posterior to high flow events and related to systems in recovery from these events. This highlights that the suspended sediment response observed at the event scale is highly transient with little long-term effects on the sourcing and nature of the suspended matter. In a sense, this aspect corroborates the observation that solute concentration–discharge relationships at the hydrologic event scale can differ substantially from those over the long term [44].

5. Conclusions

Our analysis of the evolution of the nature of suspended sediments in three small watersheds of different lithology over one year highlighted two fundamental points: (1) bedrock geology did not significantly alter the nature of the suspended sediments in this high weathering rate system, and (2) with respect to suspended matter, all three rivers appeared highly resilient to hydrologic events. These results have implications

related to river response to events, in particular in relation to climate change. Using the year 2006 as a baseline, our analysis suggests that small tropical catchments are quite resilient to precipitation events. Although no major hurricane or tropical storm directly affected our study area during the sampling time, in all streams, numerous drought and storm events did not alter the nature of the particulate matter over the long term. Due to the fact that the suspended matter in the studied streams was dominated by secondary weathering products, our results imply that in intense weathering environments, such as tropical mountainous systems, the flux of river particulate matter is controlled in the higher reaches of the streams, with little in-stream processing or direct runoff contribution.

Supplementary Materials: The following supporting information can be downloaded at: https://www.mdpi.com/article/10.3390/min13020208/s1, Table S1a: List of analyzed samples from Rio Mameyes. Table S1b: List of analyzed samples from Rio Icacos. Table S1c: List of analyzed samples from Quebrada Sonadora. Table S2a: Date and maximum peak discharge (in m^3/s) of the top 5 discharge events for each river during the study period; Table S2b: Date and average daily discharge (in m^3/s) of the top 5 daily discharge events for each river during the study period; Figure S1: Grab sample sediments texture diagram.; Figure S2: XRD Diffractograms (black) and quantitative models (colors) of bulk sediment grab samples collected from the three rivers in January 2022; Figure S3: XRD Diffractograms (black) and quantitative models (colors) of the <50 μm fraction of sediment grab samples collected from the three rivers in January 2022.

References

1. Lyons, W.B.; Nezat, C.A.; Carey, A.E.; Hicks, D.M. Organic Carbon Fluxes to the Ocean from High-Standing Islands. *Geology* **2002**, *30*, 443–446. [CrossRef]
2. Buss, H.L.; White, A.F. Weathering Processes in the Icacos and Mameyes Watersheds in Eastern Puerto Rico. In *Water Quality and Landscape Processes of Four Watersheds in Eastern Puerto Rico*; Murphy, S.F., Stallard, R.F., Eds.; Professional Paper 1789-A; U.S. Geological Survey: Reston, VA, USA, 2012; Volume 14.
3. Vichot-Llano, A.; Martinez-Castro, D.; Bezanilla-Morlot, A.; Centella-Artola, A.; Giorgi, F. Projected Changes in Precipitation and Temperature Regimes and Extremes over the Caribbean and Central America Using a Multiparameter Ensemble OfRegCM4. *Int. J. Climatol.* **2021**, *41*, 1328–1350. [CrossRef]
4. Clark, K.E.; Shanley, J.B.; Scholl, M.A.; Perdrial, N.; Perdrial, J.N.; Plante, A.F.; McDowell, W.H. Tropical River Suspended Sediment and Solute Dynamics in Storms during an Extreme Drought. *WATER Resour. Res.* **2017**, *53*, 3695–3712. [CrossRef]
5. Stocker, T.F.; Qin, D.; Plattner, G.-K.; Tignor, M.; Allen, S.K.; Boschung, J.; Nauels, A.; Xia, Y.; Bex, V.; Midgley, P.M. *IPCC, 2013: Climate Change 2013: The Physical Science Basis. Contribution of Working Group I to the Fifth Assessment Report of the Climate Change*; Cambridge University Press: Cambridge, UK; New York, NY, USA, 2013; p. 1535.
6. Jahandideh-Tehrani, M.; Zhang, H.; Helfer, F.; Yu, Y. Review of Climate Change Impacts on Predicted River Streamflow in Tropical Rivers. *Environ. Monit. Assess.* **2019**, *191*, 752. [CrossRef]
7. Siddha, S.; Sahu, P. Chapter 5—Impact of Climate Change on the River Ecosystem. In *Ecological Significance of River Ecosystems*; Madhav, S., Kanhaiya, S., Srivastav, A., Singh, V., Singh, P., Eds.; Elsevier: Amsterdam, The Netherlands, 2022; pp. 79–104. ISBN 978-0-323-85045-2.

8.   Hauer, C.; Leitner, P.; Unfer, G.; Pulg, U.; Habersack, H.; Graf, W. The Role of Sediment and Sediment Dynamics in the Aquatic Environment. In *Riverine Ecosystem Management*; Schmutz, S., Sendzimir, J., Eds.; Aquatic Ecology Series; Springer: Cham, Switzerland, 2018.

9.   Chakrapani, G.J. Factors Controlling Variations in River Sediment Loads. *Curr. Sci.* **2005**, *88*, 569–575.

10.   Viers, J.; Dupré, B.; Gaillardet, J. Chemical Composition of Suspended Sediments in World Rivers: New Insights from a New Database. *Sci. Total Environ.* **2009**, *407*, 853–868. [CrossRef] [PubMed]

11.   Garzanti, E.; Andó, S.; France-Lanord, C.; Censi, P.; Vignola, P.; Galy, V.; Lupker, M. Mineralogical and chemical variability of fluvial sediments 2. Suspended-load silt (Ganga–Brahmaputra, Bangladesh). *Earth Planet. Sci. Lett.* **2011**, *302*, 107–120. [CrossRef]

12.   Galloway, J.N.; Dentener, F.J.; Capone, D.G.; Boyer, E.W.; Howarth, R.W.; Seitzinger, S.P.; Asner, G.P.; Cleveland, C.C.; Green, P.A.; Holland, E.A.; et al. Nitrogen Cycles: Past, Present, and Future. *Biogeochemistry* **2004**, *70*, 153–226. [CrossRef]

13.   Meybeck, M. Global Analysis of River Systems: From Earth System Controls to Anthropocene Syndromes. *Philos. Trans. R. Soc. B-Biol. Sci.* **2003**, *358*, 1935–1955. [CrossRef] [PubMed]

14.   Martin, J.-M.; Meybeck, M. Elemental Mass-Balance of Material Carried by Major World Rivers. *Mar. Chem.* **1979**, *7*, 173–206. [CrossRef]

15.   Meybeck, M. Global Chemical-Weathering of Surficial Rocks Estimated from River Dissolved Loads. *Am. J. Sci.* **1987**, *287*, 401–428. [CrossRef]

16.   Gaillardet, J.; Dupre, B.; Louvat, P.; Allegre, C.J. Global Silicate Weathering and CO2 Consumption Rates Deduced from the Chemistry of Large Rivers. *Chem. Geol.* **1999**, *159*, 3–30. [CrossRef]

17.   White, A.; Blum, A. Effects of Climate on Chemical-Weathering in Watersheds. *Geochim. Cosmochim. Acta* **1995**, *59*, 1729–1747. [CrossRef]

18.   Goldsmith, S.T.; Moyer, R.P.; Harmon, R.J. Hydrochemistry and Biogeochemistry of Tropical Small Mountain Rivers. *Appl. Geochem.* **2015**, *63*, 453–455. [CrossRef]

19.   Dinis, P.A.; Garzanti, E.; Hahn, A.; Vermeesch, P.; Cabral-Pinto, M. Weathering Indices as Climate Proxies. A Step Forward Based on Congo and SW African River Muds. *Earth-Sci. Rev.* **2020**, *201*, 103039. [CrossRef]

20.   He, J.; Garzanti, E.; Dinis, P.; Yang, S.; Wang, H. Provenance versus Weathering Control on Sediment Composition in Tropical Monsoonal Climate (South China)-1. Geochemistry and Clay Mineralogy. *Chem. Geol.* **2020**, *558*, 119860. [CrossRef]

21.   Solano-Rivera, V.; Geris, J.; Granados-Bolaños, S.; Brenes-Cambronero, L.; Artavia-Rodríguez, G.; Sánchez-Murillo, R.; Birkel, C. Exploring Extreme Rainfall Impacts on Flow and Turbidity Dynamics in a Steep, Pristine and Tropical Volcanic Catchment. *Catena* **2019**, *182*, 104118. [CrossRef]

22.   Kimeli, A.; Ocholla, O.; Okello, J.; Koedam, N.; Westphal, H.; Kairo, J. Geochemical and Petrographic Characteristics of Sediments along the Transboundary (Kenya–Tanzania) Umba River as Indicators of Provenance and Weathering. *Open Geosci.* **2021**, *13*, 1064–1083. [CrossRef]

23.   Li, L.; Ni, J.; Chang, F.; Yue, Y.; Frolova, N.; Magritsky, D.; Borthwick, A.G.L.; Ciais, P.; Wang, Y.; Zheng, C.; et al. Global Trends in Water and Sediment Fluxes of the World's Large Rivers. *Sci. Bull.* **2020**, *65*, 62–69. [CrossRef]

24.   Syvitski, J.P.M.; Cohen, S.; Kettner, A.J.; Brakenridge, G.R. How Important and Different Are Tropical Rivers?—An Overview. *Geomorphology* **2014**, *227*, 5–17. [CrossRef]

25.   Keellings, D.; Hernández Ayala, J.J. Extreme Rainfall Associated with Hurricane Maria over Puerto Rico and Its Connections to Climate Variability and Change. *Geophys. Res. Lett.* **2019**, *46*, 2964–2973. [CrossRef]

26.   Dang, T.D.; Cochrane, T.A.; Arias, M.E.; Van, P.D.T.; de Vries, T.T. Hydrological Alterations from Water Infrastructure Development in the Mekong Floodplains. *Hydrol. Process.* **2016**, *30*, 3824–3838. [CrossRef]

27.   Ramos-Scharron, C.E.; Garnett, C.T.; Arima, E.Y. A Catalogue of Tropical Cyclone Induced Instantaneous Peak Flows Recorded in Puerto Rico and a Comparison with the World's Maxima. *Hydrology* **2021**, *8*, 84. [CrossRef]

28.   Hynek, S.A.; McDowell, W.H.; Bhatt, M.P.; Orlando, J.J.; Brantley, S.L. Lithological Control of Stream Chemistry in the Luquillo Mountains, Puerto Rico. *Front. Earth Sci.* **2022**, *10*, 414. [CrossRef]

29.   Murphy, S.F.; Stallard, R.F. Hydrology and Climate of Four Watersheds in Eastern Puerto Rico. In *Water Quality and Landscape Processes of Four Watersheds in Eastern Puerto Rico*; Murphy, S.F., Stallard, R.F., Eds.; Professional Paper 1789-A; U.S. Geological Survey: Reston, VA, USA, 2012; Volume 42.

30.   McDowell, W.H.; Scatena, F.N.; Waide, R.B.; Brokaw, N.; Camilo, G.R.; Covich, A.P.; Crowl, T.A.; González, G.; Greathouse, E.A.; Klawinski, P.; et al. Geographic and Ecological Setting of the Luquillo Mountains. In *A Caribbean Forest Tapestry*; Oxford University Press: New York, NY, USA, 2012; ISBN 978-0-19-533469-2.

31.   Murphy, S.F.; Stallard, R.F.; Larsen, M.C.; Gould, W.A. Physiography, Geology, and Land Cover of Four Watersheds in Eastern Puerto Rico. In *Water Quality and Landscape Processes of Four Watersheds in Eastern Puerto Rico*; Murphy, S.F., Stallard, R.F., Eds.; Professional Paper 1789-A; U.S. Geological Survey: Reston, VA, USA, 2012; Volume 24.

32.   Lidiak, E.G.; Larue, D.K. *Tectonics and Geochemistry of the Northeastern Caribbean*; Geological Society of America: Boulder, CO, USA, 1998; ISBN 978-0-8137-2322-8.

33.   Seiders, V.M. Geologic Map of the El Yunque Quadrangle, Puerto Rico. *IMAP* **1971**, 658. [CrossRef]

34.   Buss, H.L.; Sak, P.B.; Webb, S.M.; Brantley, S.L. Weathering of the Rio Blanco Quartz Diorite, Luquillo Mountains, Puerto Rico: Coupling Oxidation, Dissolution, and Fracturing. *Geochim. Cosmochim. Acta* **2008**, *72*, 4488–4507. [CrossRef]

35. Fletcher, R.C.; Buss, H.L.; Brantley, S.L. A Spheroidal Weathering Model Coupling Porewater Chemistry to Soil Thicknesses during Steady-State Denudation. *Earth Planet. Sci. Lett.* **2006**, *244*, 444–457. [CrossRef]
36. Simon, A.; Larsen, M.C.; Hupp, C.R. The Role of Soil Processes in Determining Mechanisms of Slope Failure and Hillslope Development in a Humid-Tropical Forest Eastern Puerto Rico. *Geomorphology* **1990**, *3*, 263–286. [CrossRef]
37. Briggs, R.P. *The Lower Cretaceous Figuera Lava and Fajardo Formation in the Stratigraphy of Northeastern Puerto Rico*; Geological Survey Bulletin; For Sale by the Superintendent of Documents, US Government Printing Office: Washington, DC, USA, 1973.
38. McDowell, W.; Brereton, R.; Scatena, F.; Shanley, J.; Brokaw, N.; Lugo, A. Interactions between Lithology and Biology Drive the Long-Term Response of Stream Chemistry to Major Hurricanes in a Tropical Landscape. *Biogeochemistry* **2013**, *116*, 175–186. [CrossRef]
39. Perdrial, N.; Thompson, A.; O'Day, P.A.; Steefel, C.I.; Chorover, J. Mineral Transformation Controls Speciation and Pore-Fluid Transmission of Contaminants in Waste-Weathered Hanford Sediments. *Geochim. Cosmochim. ACTA* **2014**, *141*, 487–507. [CrossRef]
40. Rietveld, H.M. A Profile Refinement Method for Nuclear and Magnetic Structures. *J. Appl. Crystallogr.* **1969**, *2*, 65–71. [CrossRef]
41. Warr, L.N. IMA–CNMNC Approved Mineral Symbols. *Mineral. Mag.* **2021**, *85*, 291–320. [CrossRef]
42. Velbel, M.A. Bond Strength and the Relative Weathering Rates of Simple Orthosilicates. *Am. J. Sci.* **1999**, *299*, 679–696. [CrossRef]
43. Gordeev, V.V.; Dara, O.M.; Filippov, A.S.; Belorukov, S.K.; Lokhov, A.S.; Kotova, E.I.; Kochenkova, A.I. Mineralogy of Particulate Suspended Matter of the Severnaya Dvina River (White Sea, Russia). *Minerals* **2022**, *12*, 1600. [CrossRef]
44. Knapp, J.L.A.; von Freyberg, J.; Studer, B.; Kiewiet, L.; Kirchner, J.W. Concentration–Discharge Relationships Vary among Hydrological Events, Reflecting Differences in Event Characteristics. *Hydrol. Earth Syst. Sci.* **2020**, *24*, 2561–2576. [CrossRef]
45. Neubauer, E.; Köhler, S.J.; von der Kammer, F.; Laudon, H.; Hofmann, T. Effect of PH and Stream Order on Iron and Arsenic Speciation in Boreal Catchments. *Environ. Sci. Technol.* **2013**, *47*, 7120–7128. [CrossRef]
46. Le Meur, M.; Montargès-Pelletier, E.; Bauer, A.; Gley, R.; Migot, S.; Barres, O.; Delus, C.; Villiéras, F. Characterization of Suspended Particulate Matter in the Moselle River (Lorraine, France): Evolution along the Course of the River and in Different Hydrologic Regimes. *J. Soils Sediments* **2016**, *16*, 1625–1642. [CrossRef]
47. Van Put, A.; Van Grieken, R.; Wilken, R.-D.; Hudec, B. Geochemical Characterization of Suspended Matter and Sediment Samples from the Elbe River by EPXMA. *Water Res.* **1994**, *28*, 643–655. [CrossRef]
48. Matsunaga, T.; Tsuduki, K.; Yanase, N.; Kritsananuwat, R.; Ueno, T.; Hanzawa, Y.; Naganawa, H. Temporal Variations in Metal Enrichment in Suspended Particulate Matter during Rainfall Events in a Rural Stream. *Limnology* **2014**, *15*, 13–25. [CrossRef]
49. Nagano, T.; Yanase, N.; Tsuduki, K.; Nagao, S. Particulate and Dissolved Elemental Loads in the Kuji River Related to Discharge Rate. *Environ. Int.* **2003**, *28*, 649–658. [CrossRef]